Topics in Catalysis (2020) 63:1227–1239
https://doi.org/10.1007/s11244-020-01364-2

ORIGINAL PAPER

Enhanced Photocatalytic Degradation of MB Under Visible Light Using the Modified MIL-53(Fe)

Tran Thuong Quang[1] · Nguyen Xuan Truong[1] · Tran Hong Minh[1] · Nguyen Ngoc Tue[1] · Giang Thi Phuong Ly[1]

Published online: 3 September 2020
© Springer Science+Business Media, LLC, part of Springer Nature 2020

Abstract

In this report, we focus on the modification of iron terephthalate metal–organic framework (MIL-53(Fe)) by soaking in H_2O_2 solution and its mechanism. The structure of MIL-53(Fe) before and after the modification were characterized by Fourier-transform infrared spectroscopy (FTIR), X-ray powder diffraction (XRD), and N_2 adsorption–desorption isotherms. The XRD results showed that the material structure changed to amorphous phases and the photocatalytic efficiency was improved after modified by H_2O_2. The MIL-53 (Fe, H_2O_2) nanoparticles about 100–300 nm in size was successfully prepared and confirmed by SEM images. In term of UV–Vis DRS results, the absorption spectrum of modified MIL-53(Fe) shifted to higher wavelength and its band gap energy is estimated about 2.2 eV, which is significantly lower than the bandgap value of the conventional material. The impact of the modification on the photocatalytic efficiency was investigated by methylene blue (MB) degradation experiments and photoluminescence (PL) spectroscopy. MB was completely decomposed within 30 min by modified MIL-53(Fe) under optimal conditions. The reaction parameters that affect MB degradation by the as-prepared catalyst were also investigated, including the pH solution, catalyst and H_2O_2 dosage.

Keywords MIL-53(Fe) · Photocatalyst · Fenton oxidation · MB degradation

1 Introduction

Advanced oxidation processes (AOPs) are alternative techniques for environmental redemption in which contaminants are breakdown by a powerful oxidizing species such as hydroxyl radicals (·OH), superoxide radical ($O_2^{\cdot-}$), etc. Heterogeneous photocatalyst-assisted AOPs have emerged as a potential solution for water, air, and wastewater treatment and energy generation. Among the hazardous substances that contaminate water, synthetic dyes are the most difficult to remove due to their complex aromatic structure, which makes them resistant to oxidation, biodegradation, temperature and light irradiation [1]. On top of that, some dyes possess toxicity, multagenic, and/or carcinogenic effects, which damages the health of human being and other living creatures [1, 2].

Metal organic framework (MOFs) are composed of metal ions/clusters and multifunctional organic bridging ligands have received much attention recently. Crystalline metal–organic frameworks (*c*MOFs) have widespread applications owing to their superb features including low densities, high surface areas, tunable pore size, and high porosities. Along with the rapid development of *c*MOFs, amorphous MOFs (*a*MOFs), which maintain the basic building blocks but without long-range crystallinity, have emerged recently [3]. Compared to *c*MOFs, *a*MOFs exhibited higher conductivity, more defective sites and improved photoluminescence efficiency [4]. In previous reports, *a*MOFs were synthesized using high-temperature heating [5], high-energy ball-milling [6], pressurizing (~ 1 GPa) [7] or electron-beam-induced amorphization procedures [8], and their applications are focused mainly in adsorption, separation and drug delivery.

The excited metal clusters working as the main active sites of photocatalytic reaction have a great influence on catalytic performance the MOFs. It is the reason why choosing the appropriate metal cluster is essential to construct the MOFs with high activity [9]. The Fe-containing MOF materials, which have Fe oxo-cluster as the core, show themselves to be a promising catalyst for contaminant decomposition purposes owing to their superior characteristics such

✉ Tran Thuong Quang
quang.tranthuong@hust.edu.vn

[1] School of Chemical Engineering, Hanoi University of Science and Technology, Hanoi, Vietnam

as catalytic activity followed semiconductors mechanism or Fenton mechanism, stability, simple synthesis method, etc. MIL-53(Fe), which is a typical Fe-containing MOF material, was built upon infinite one-dimensional linkage of –Fe–O–O–Fe–O–Fe–, cross-linked by 1,4-benzenedicarboxylate (BDC) ligands [10]. In addition to the photocatalytic ability, this MOF also owns a flexible structure which enables it to open/close its pores in order to adsorb/desorb guest molecules even though its surface area is not as large as those of other MOFs. MIL-53(Fe) has been studied for various applications such as gas adsorption [11], liquid phase adsorption [12], sensors [13] and photocatalytic degradation contaminants [14].

Recently, many reports have focused on the aspect of modifying MOFs for finding better photocatalytic performance or the improvement of stability. Some typical strategies for modifying MOFs can be mentioned such as the use of functional group modified linkers, microwave or/and ultrasonic assisted method, the creation of nanocomposite materials with semiconductor materials, control particles size by polymers/surfactants, etc. In using functional-group-decorated ligands strategy, amine substituted linkers are commonly chosen owing to its strong electron-donating capacity which leads to a drop on bandgap energy of materials. For example, Hu et al. successfully prepared amine functionalized ZIF-8 by stirring the conventional ZIF-8 in ethylenediamine (EDA) with different ZIF-8/EDA ratios, and the results showed that when the EDA molar ratio increased, the obtained samples exhibited enhanced light absorption in the range of 300–500 nm [15]. In addition, the other functional groups such as –OH, $–CH_3$, –Cl can also reduce the band gap value, but the effects of those are less than that of $–NH_2$ substitution [9]. Microwave and ultrasonic assisted method are employed to produced MOFs in shorter period and at lower temperature, aiming to reduce energy consumption [16, 17]. Contained MOFs nanocomposite materials such as Fe_3O_4/MOFs, g-C_3N_4/MOFs, GO/MOFs, C-dots etc. whose nano-objects are semiconductors that can be activated by visible light, emerged as a class of hybrid materials possessing superior characteristics [18–22]. Typical characteristics include high porosity with ordered crystalline pores and high surface areas contribute to the uniform dispersion and the high density of catalytic sites, which can enhance the catalytic efficiency [23]. Controlling MOFs particles with polymers/surfactants strategy requires the suitable polymers/surfactants, whose characteristics significantly affect the size and shape of the MOFs nanoparticles. Polymers such as polyethylene glycol (PEG) and polyvinyl pyrrolidone (PVP) are usually chosen to modulate the particle growth and/or shape, and they sometimes go into the skeleton of the MOFs and become part of the MOF materials [24]. The advantage of this method is to synthesis uniform nanoscale MOFs particles with size parameter is smaller than 100 nm.

The metal–organic frameworks MIL-53(Fe) can be purified by using hydrogen peroxide, reported by Nguyen et al. [25]. In a word, with the presence of hydrogen peroxide at concentration of 75 mM in aqueous solution and with exposure under UVA–Vis irradiation for 1 h, organic impurities were decomposed completely without damage of MIL-53(Fe) structure. The effects of hydrogen peroxide concentration also were investigated; in an hour of treatment, the higher concentration of hydrogen peroxide, the more efficient purification. The result shown both the free 1,4-H_2BDC and confined 1,4-H_2BDC were almost destroyed. A question for this process is with higher concentration of H_2O_2 and longer immersion time, the OH radical will affect to the linker or not and the structure will be changed or not? In this work, as-prepared MIL-53(Fe) was suspending into a 1 M H_2O_2 solution for 24 h. The structure of MIL-53(Fe) have been changed from the crystalline MIL-53(Fe) to amorphous MIL-53(Fe) under high concentration of H_2O_2. To confirm the hypothesis, characteristic features of both materials were examined by Fourier-transform infrared spectroscopy (FTIR), X-ray powder diffraction (XRD), UV–Vis diffuse reflectance (UV–Vis DRS), N_2 adsorption–desorption isotherms. Moreover, the photocatalytic efficiency of modified and conventional MIL-53(Fe) were investigated by Methylene Blue (MB) degradation and the detection of hydroxy radical ·OH formation during the experiments. MB was selected as the model organic contaminant owing to its stable molecular structure as well as its widespread presence in effluent. The reaction parameters that affect MB degradation by the as-prepared catalyst were also determined, including the pH solution, catalyst and H_2O_2 external dosage.

2 Experimental

2.1 Chemicals and Reagents

All chemicals and reagents were obtained from commercial suppliers and used without further purification. Ferric chloride hexahydrate (> 99%, $FeCl_3·6H_2O$), Terephthalic acid (1,4-BDC, > 98%), dimethylformamide (DMF, > 99%), methylene blue (MB, > 99%), Hydroperoxide solution (H_2O_2, 30%, v/v), Hydrochloric acid (HCl, 36–38%) and Sodium hydroxide (NaOH, > 96%) were purchased from Xilong Scientific Company located in Shantou, Guangdong, China. Distilled water was used for all test experiments.

2.2 Preparation and Modification of MIL-53(Fe)

The modified MIL-53(Fe) was prepared from the conventional MIL-53(Fe), which was synthesized via solvothermal method reported by Ai et al. [26] with some differences. Briefly, 5 mmol $FeCl_3·6H_2O$ and 1 mmol terephthalic acid

were added slowly to 25 mL DMF as the solvent. The mixture was then stirred and ultrasonicated at ambient conditions until completely dissolved. The obtain light yellow mixture was subsequently transferred into a stainless autoclave for heat treatment at 140 °C for 5 h. After the heat treatment, the autoclave was cooled down to room temperature. The solvent was then removed by a vacuum filter and the obtained solid was continually washed with 150 mL of distill water. The obtained conventional MIL-53(Fe) was dried in the vacuum at 70 °C for 2 h and 150 °C for 3 h. The modified MIL-53(Fe) was prepared by suspending the conventional product into a dilute H_2O_2 solution for 24 h and then was dried again with the same procedure as described. The brown material obtained after H_2O_2 treatment was named MIL-53(Fe, H_2O_2) to distinguish it from conventional MIL-53(Fe).

2.3 Characterization

XRD patterns was obtained by a Bruker D8 Discovery X-ray Diffractometer using Ni-filtered Cu–Kα radiation (λ = 0.154056 nm) as the X-ray source. The recorded range of 2θ was from 5° to 45° and the scanning rate was set at 4° per min. The FTIR spectra were obtained by a JASCO FT/IR6300 Spectrometric Analyzer in the range from 400 to 4000 cm^{-1} at room temperature. The morphology of samples was observed with a JEOL JMS-7600F scanning electron microscope (SEM). UV–Vis diffuse reflectance spectra (UV–Vis DRS) were obtained by a JACO V-670 UV–Vis spectrophotometer with $BaSO_4$ as a reflectance standard. The Brunauer–Emmett–Teller (BET) surface areas and pore size distribution of the samples were determined on a TriStar 3000 V6.07A at 77 K using nitrogen adsorbate.

2.4 Catalytic Degradation Experiments

For catalytic performance comparison, MB degradation experiments were conducted under visible light. In details, 10 mg of MOF powder was suspended into 50 mL of 10 mg L^{-1} MB aqueous solution by magnetic stir at ambient conditions. Next, the reaction mixture was kept in the dark for 30 min to establish the adsorption/desorption equilibrium. After 30 min, the mixture was taken out to the visible light and subsequently added a known concentration of H_2O_2. The visible light was created by a 500 W halogen tungsten lamp through a UV-cutoff filter (420 nm). Dye concentration in centrifugal liquids was investigated by Hatch UV–Vis spectrophotometer model DR 3900 with a 1 cm quartz cell every 10 min.

Beside comparing photocatalytic performances, various experiments in different conditions were conducted to deeply understand the ability degradation of MIL-53(Fe, H_2O_2). The studied reaction parameters that affect the MB degradation by the as-prepared catalyst was the initial pH of dye solution, catalyst and H_2O_2 dosage. To determine the stability of MIL-53(Fe, H_2O_2), the material was recovered from the resulting MB aqueous by centrifugation and reused for subsequent reactions.

2.5 Hydroxyl Radical Detection Experiments

The photoluminescence (PL) spectroscopy was employed to inspect the formation of hydroxyl radical ·OH in order to provide a further proof of the effect of the modification step. Terephthalic acid was selected as a fluorescence probe [26–28]. The experimental procedures were the same as those used in the catalytic experiments except that the aqueous solution of MB was replaced by an aqueous solution of 0.6 mM terephthalic acid and 2 mM NaOH. Briefly, 5 mg of MOF powder was suspended into 25 mL solution containing 0.6 mM terephthalic acid and 2 mM NaOH by magnetic stirring. The mixture was then left under visible light, and H_2O_2 was not used in this kind of experiments. The PL intensity of the solution was analyzed every 5 min by a RF-5301PC Shimadzu fluorescence spectrophotometer at 315 nm of excitation wavelength with a 1 cm quartz cuvette.

3 Results and Discussion

3.1 Structure and Morphology of Modified and Conventional MIL-53(Fe) Materials

The XRD patterns of MIL-53(Fe) and MIL-53(Fe, H_2O_2) are shown in Fig. 1a. In the red curve, the main diffraction peaks appearing at 2θ of 9.10, 12.54, 17.50, 17.94, 17.98, 25.32, 27.12, 29.58, 30.00, 36.28 are identical to those peaks reported for the MIL-53(Fe) phases as well as those in the stimulation pattern, which confirms the high crystallinity of the conventional sample [26, 29]. However, no peak is observed in the blue curve (Fig. 1a), it suggests that the modification changed the crystal structure into the amorphous one of the materials. Moreover, the FTIR spectra of these MOFs are shown in Fig. 1b. The absorption features of the conventional MIL-53(Fe) sample at 1622.13, 1523.76, 1375.25, 748.38, and 524.64 cm^{-1} are consistent with reported data [26, 29]. As seen in Fig. 1b, the FTIR spectrum of MIL-53(Fe, H_2O_2) is similar to that of MIL-53(Fe). The two intense peaks at 1568.13 and 1384.89 cm^{-1} are attributed to asymmetric (ϑ_{as}(C–O)) and symmetric (ϑ_s(C–O)) vibrations of carboxyl groups, respectively. The C–H stretching vibrations of benzene are represented by a sharp peak at 746.45 cm^{-1}. The absorption peak at 534.2 cm^{-1} can be assigned to the Fe–O vibrations. It reveals that the backbone of the MIL-53(Fe) structure remained after the modification step.

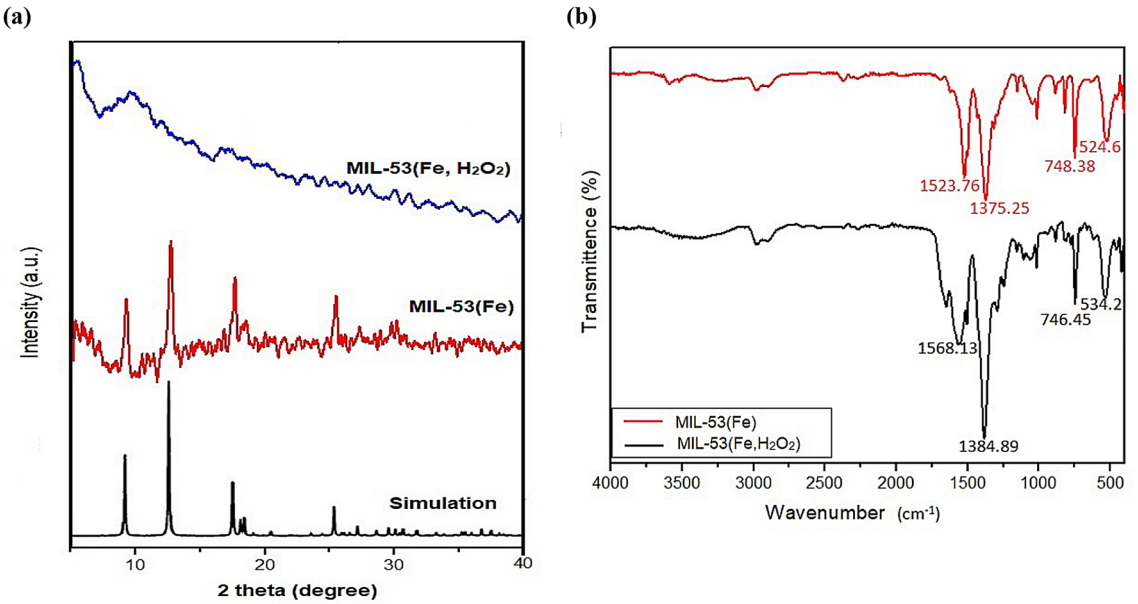

Fig. 1 XRD patterns (**a**) and FTIR spectrum (**b**) of MIL-53(Fe) and MIL-53(Fe, H_2O_2)

The morphology features and particle size of MIL-53(Fe) and modified MIL-53(Fe) were investigated by the scanning electron microscopy (SEM) and the results are shown in Fig. 2. Figure 2a indicates that MIL-53(Fe) has a rod-like structure with an average size of 4 μm in width [26]. Modified MIL-53(Fe) are nanoparticles about 100–300 nm in size (Fig. 2c, d).

The porous properties of MIL-53(Fe) and MIL-53(Fe, H_2O_2) was compared to each other by N_2 adsorption–desorption isotherms at 77 K, and the full data is illustrated in

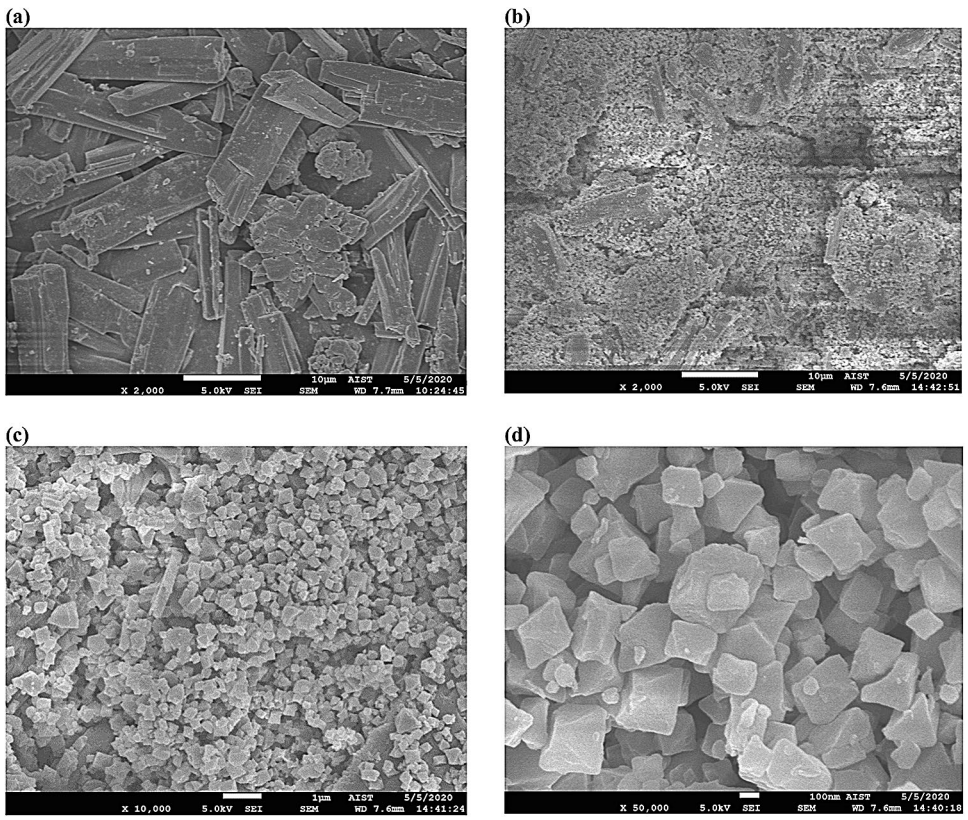

Fig. 2 SEM images of (**a**) MIL-53 (Fe) and (**b**–**d**) MIL-53(Fe, H_2O_2)

Table 1 and Fig. 3. In term of BET surface area, the value of modified MIL-53(Fe) is 8.93 $m^2 g^{-1}$, which is slightly lower than the data of conventional one. The average pore size of MIL-53(Fe, H_2O_2) is also smaller than that of MIL-53(Fe), however, the pore volume of MIL-53(Fe, H_2O_2) is higher than that of MIL-53(Fe). As a comparison, the reported BET surface areas and pore sizes of MIL-53(Fe) from other literature were also provided in Table 2. It is evidence that MIL-53(Fe) synthesized under different conditions possesses quite different BET surface areas.

The optical properties of the conventional and modified MIL-53 (Fe) were examined by UV–Vis diffuse reflectance spectroscopy (Fig. 4a) and their bandgap values were estimated by using the Tauc plot (Fig. 4b). MIL-53(Fe) behaves strong visible light absorption in the range of 200–400 nm, which is a good agreement with the previous reports [26, 30]. Based on the relation Eg = 1240/λ, the calculated optical band gap of MIL-53(Fe) is 2.72 eV (Fig. 5b) [26, 30]. Meanwhile, the background absorption of MIL-53(Fe, H_2O_2) surprisingly enhances and its bandgap value is dropped to 2.2 eV. This result is consistent with the color change of material MIL-53(Fe) after the H_2O_2 treatment, in which the solid's color changed from light orange to dark brown. It is evidence that the photocatalytic performance of MIL-53(Fe) is enhanced to a certain degree.

Table 1 Specific surface area and porous structure of MIL-53(Fe) and MIL-53(Fe, H_2O_2)

Samples	BET surface area[a] ($m^2 g^{-1}$)	Pore volume[b] ($cm^3 g^{-1}$)	Pore size (nm)[c]
MIL-53(Fe)	9.77	0.03	34.13
MIL-53(Fe, H_2O_2)	8.93	0.04	34.08

[a]BET specific surface

[b]Total pore volume measured at $P/P_o = 0.99$

[c]The pore diameter calculated from the absorption branch of the isotherm using the BJH method

3.2 The Photocatalytic Activity of Modified and Conventional MIL-53(Fe) Materials

Firstly, MIL-53(Fe) was compared to MIL-53(Fe, H_2O_2) in term of the photocatalytic performance by conducting MB degradation experiments. Two investigated systems were MOF/H_2O_2/vis and MOF/H_2O_2/dark, with MB's concentration of 10 mg L^{-1}, initial pH of 7 and 10 mg MOF catalyst. It is noted that the amount of H_2O_2 was used as 0.01 mM for all experiments, which was less than previous studies on MIL-53(Fe) or Fe-containing MOFs [20, 26, 27]. Before adding H_2O_2, all experiments were kept in the dark in 30 min to establish the adsorption/desorption equilibrium. For the MOF/H_2O_2/vis system (Fig. 5a), it was found that the degradation efficiency of MB with MIL-53(Fe, H_2O_2) reached 97.5% within 30 min while only 47.5% MB removal with MIL-53(Fe) supports in 60 min. It means the modified MIL-53(Fe) material indeed exhibits stronger activity than the original one. For the MOF/H_2O_2/dark system plotted (Fig. 5b), the similar behavior was observed, MB was fully decomposed within 60 min with MIL-53(Fe, H_2O_2) while only 40% MB degradation with MIL-53(Fe). This supports the idea that the catalytic activity of MIL-53(Fe) can be improved by the modification and the required amount of H_2O_2 can be reduced for each degradation experiment. The optimal reaction conditions will be discussed in the later part of this study.

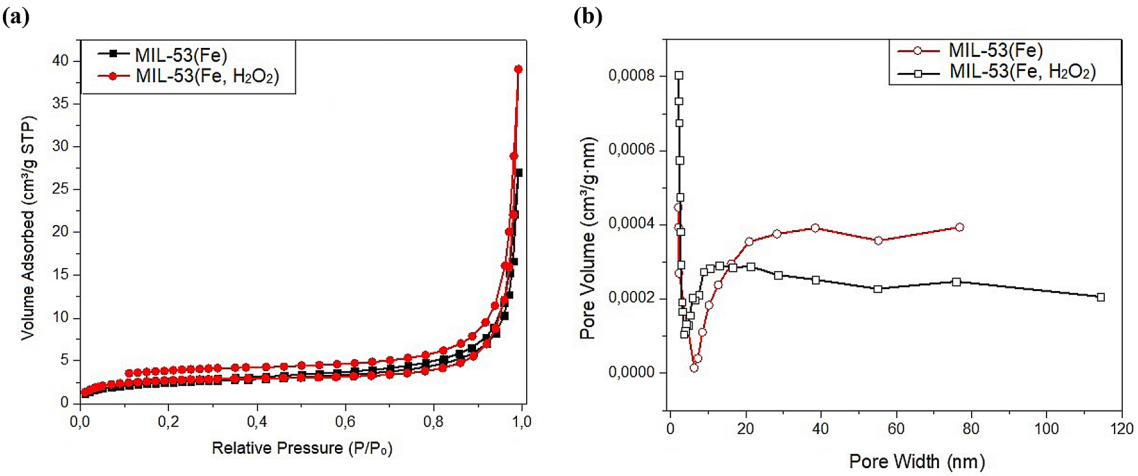

Fig. 3 **a** Nitrogen adsorption–desorption isotherms of MIL-53(Fe) and MIL-53(Fe, H_2O_2). **b** The Barrett–Joyner–Halenda (BJH) mesoporous size distribution of MIL-53(Fe) and MIL-53(Fe, H_2O_2)

Table 2 Structure properties of MIL-53(Fe) compared under different synthesis conditions

Samples name	Materials	Temperature (°C) Time (h)	S_{BET} ($m^2 g^{-1}$)	Total pore volume ($cm^3 g^{-1} \times 10^{-2}$)	Pore size (nm)	References
MIL-53(Fe)	$FeCl_3.6H_2O$ (5 mmol) 1,4-BDC (5 mmol) DMF (25 mL)	140 °C-5 h	9.77	3.14	34.13	This study
MIL-53(Fe)-A	$FeCl_3.6H_2O$ (5 mmol) 1,4-BDC (5 mmol) DMF (25 mL)	150 °C-5 h	88.64	12.06	3.03	[35]
MIL-53(Fe)-E	$FeCl_3.6H_2O$ (5 mmol) 1,4-BDC (5 mmol) DMF (25 mL)	150 °C-8 h	7.45	2.19	8.80	[35]
MIL-53(Fe)-F	$FeCl_3.6H_2O$ (5 mmol) 1,4-BDC (5 mmol) DMF (25 mL)	150 °C-10 h	6.80	1.82	10.73	[35]
MIL-53(Fe)-G	$FeCl_3.6H_2O$ (5 mmol) 1,4-BDC (5 mmol) DMF (25 mL)	150 °C-12 h	6.48	1.60	11.73	[35]
MIL-53(Fe)-H	$FeCl_3.6H_2O$ (5 mmol) 1,4-BDC (5 mmol) DMF (25 mL)	150 °C-24 h	5.13	1.60	12.45	[35]
MIL-53(Fe)-I	$FeCl_3.6H_2O$ (5 mmol) 1,4-BDC (5 mmol) DMF (25 mL)	150 °C-48 h	5.03	1.43	12.71	[35]
MIL-53(Fe)-J	$FeCl_3.6H_2O$ (5 mmol) 1,4-BDC (5 mmol) DMF (25 mL)	150 °C-72 h	3.59	1.41	16.00	[35]
MIL-53(Fe)	$FeCl_3.6H_2O$ (1 mmol) 1,4-BDC (1 mmol) DMF (5 mL)	150 °C-2 h	19.10	4.80	–	[26]
MIL-53(Fe)	$FeCl_3.6H_2O$ (1 mmol) 1,4-BDC (1 mmol) HF (1 mmol) DMF (5 mL)	150 °C – 72 h	23.00	2.15	9.81	[1]
MIL-53(Fe)	$FeCl_3.6H_2O$ (1 mmol) 1,4-BDC (1 mmol) DMF (5 mL)	150 °C-2 h	965	–	–	[36]
MIL-53(Fe)	nFe/nH_2BDC/nDMF 1:1:30	180 °C-24 h	47.9	6.00	–	[37]
MIL-53(Fe)	nFe/nH_2BDC/nDMF 1:1.5:130	100 °C-72 h	300	12.8	13	[38]
MIL-53(Fe)	$FeCl_3.6H_2O$ (10 mmol) 1,4-BDC (10 mmol) HF (1.8 mL) DMF (26 mL)	150 °C-25 h	7.416	–	1.8	[39]

3.3 Mechanism of MIL-53(Fe) Modification by H_2O_2

Generally, photocatalysis processes of metal–organic framework base on two widely recognized mechanisms: (i) a ligand to metal charge transfer (LMCT) mechanism [31] and (ii) a metal–oxo cluster excitation [1, 26]. Previous researches on conventional MIL-53(Fe) indicated that these materials mainly followed LMCT mechanism; however, it has been verified that these materials had a low photocatalytic efficiency. Due to the poor ability in absorbing visible light of the pure organic linker (i.e. terephthalic acid), electrons cannot be excited from the valance band to the conduction band; consequently, positively charged holes and electrons cannot be generated. By using external electron acceptor (H_2O_2) which reinforced metal–oxo cluster excitation mechanism is a solution to this problem. As Ai et al. [26] reported, under the visible light irradiation, the iron–oxo cluster in MIL-53(Fe) could adsorb photons to excite electrons and thereby create positively charge holes h^+ (Eqs. 1, 2). The holes, which are strong oxidation species, could oxidize stable organic molecules. Meanwhile, H_2O_2 as an electron acceptor could capture the photoinduced

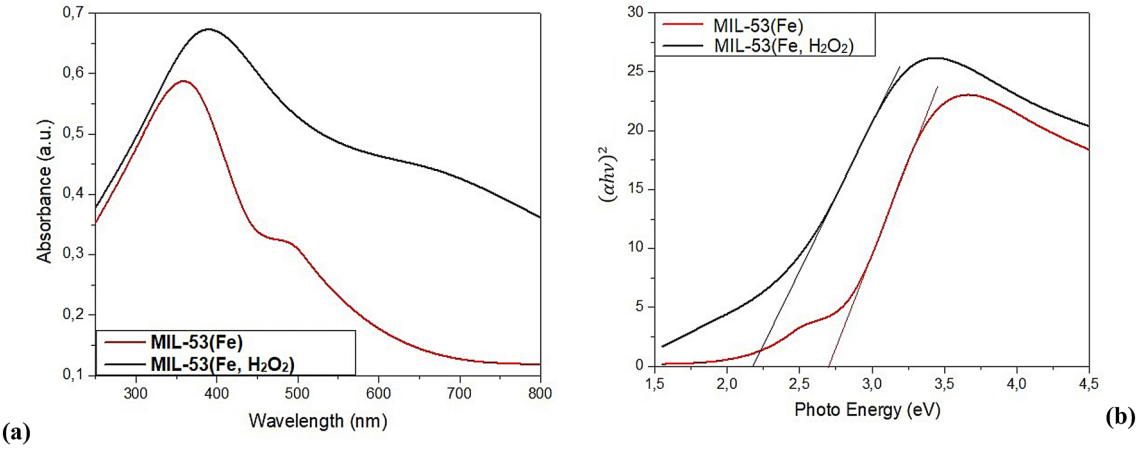

Fig. 4 **a** UV–Vis diffuse reflectance spectra of MIL-53(Fe) and MIL-53(Fe, H_2O_2). **b** The Tauc plot of $(\alpha h\nu)^2$ vs photo energy ($h\nu$) of MIL-53(Fe) and MIL-53(Fe, H_2O_2)

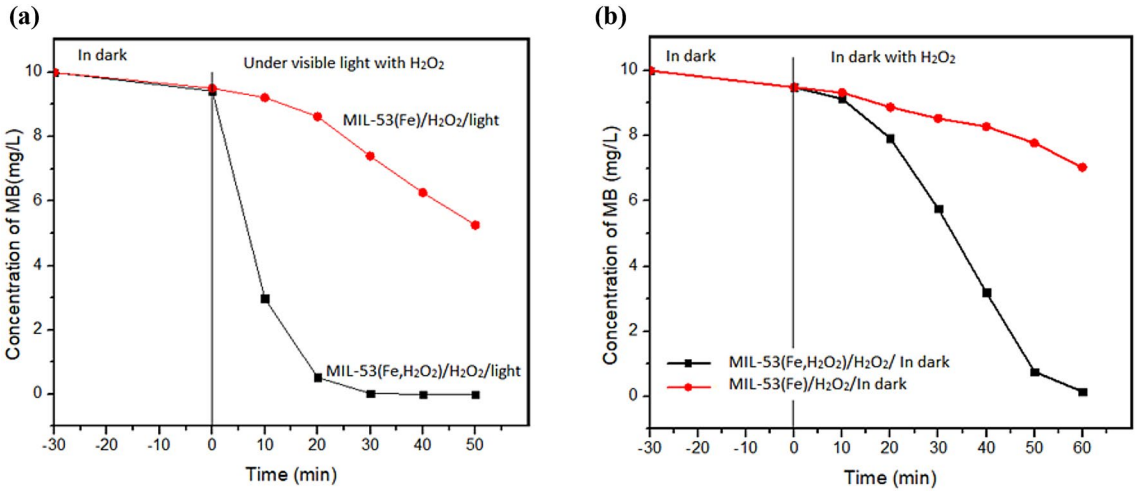

Fig. 5 MB removal by the photocatalysts in two systems **a** MOFs/H_2O_2/vis and **b** MOFs/H_2O_2/dark; (Experimental conditions: MB, 10 mg L^{-1}; H_2O_2, 0.01 mM; MOFs: 10 mg; and initial pH 7)

electrons in the excited MIL-53(Fe) to form ·OH radicals, which also have strong oxidative ability to attack stable organic molecules.

Based on the theory above, two mechanism are proposed. The first one bases on the interaction between MIL-53(Fe) and H_2O_2 to generate hydroxyl radicals ·OH. The free 1,4-H_2BDC and confined 1,4-H_2BDC were almost destroyed by ·OH, and consequently the lattice of MIL-53(Fe) was broken into many Fe cluster-BDC ligand blocks throughout the immersion procedure (Fig. 6). These blocks possessed the same backbone as the MIL-53(Fe) lattice with deflected framework and some missing-cluster/missing-linker defects and, corresponding with the FTIR results. The structural change from crystalline to amorphous was attributed to the deflected framework of Fe/BDC blocks and their random distribution in 3D space, which was consistent with the XRD results. According to De Vos et al. report, missing ligand defects result in a change of the environment of the affected transition metal atoms, which often lowers their unoccupied d-orbitals energy level [32]. Consequently, photons with greater wavelength will be able to excite electrons up to the *d*-orbital, corresponding with the significant increase in the optical absorption in the visible light region (Fig. 4a). The ·OH radical also changed the link from terephthalic acid to hydroxy terephthalic which enhanced the photocatalyst activities in visible light (Eq. 3). The new ligands are also ascribed to the narrow bandgap with stronger light absorption and excitation electronic activity [9], leading to the decrease of the amount of external H_2O_2. However, the drawback of this proposed hypothesis shows no specific signs of –OH substituent in the FTIR spectra of modified MIL-53(Fe). The second hypothesis is about the existence

of positively charged holes h^+ in the ligands after the immersion step. The holes h^+, which was generated due to the immersion in an H_2O_2 diluted solution and localized in the ligands, could attack the organic contaminants or produce ·OH without the presence of the external electron acceptor. Unlike the first hypothesis, this one cannot explain the XRD patterns in Fig. 1a. The common points of these two proposed hypotheses are that they strengthen the LMCT mechanism and reduce the amount of H_2O_2 in single degradation experiment.

$$\mathrm{MIL-53(Fe)} + \mathrm{hn} \rightarrow \mathrm{h^+ + e^-} \quad (1)$$

$$\mathrm{H_2O_2 + e^- \rightarrow {}^{\cdot}OH + OH^-} \quad (2)$$

acid react with the formed hydroxyl radicals to produce highly fluorescent compound (Eq. 4). The PL spectral changes in the MIL-53(Fe, H_2O_2)/visible light and MIL-53(Fe)/visible light systems under the same condition were recorded and shown in Fig. 7. In the case of MIL-53(Fe, H_2O_2)/light system, the intensity of the observed PL peak at about 415 nm gradually raised along with the increase in time (Fig. 7a). The change in the intensity of this peak proves the formation of ·OH radicals without the support from external H_2O_2. As shown in Fig. 7b, for the MIL-53(Fe)/visible light system, the PL intensity at ~ 415 nm does not change much, which explains ·OH radicals were hardly generated in this catalytic system. These results not only indicate that MIL-53(Fe, H_2O_2) is more active than

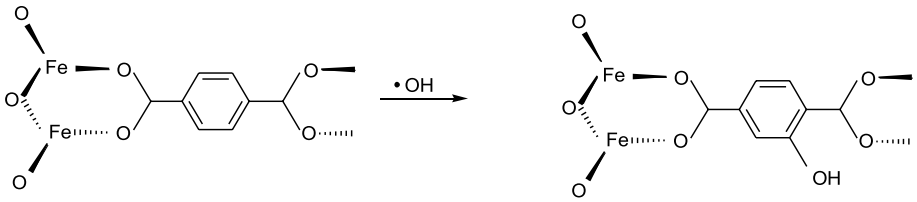

(3)

To verify the ·OH radicals formation in the MIL-53(Fe, H_2O_2)/visible light system, the PL spectroscopy was employed to detect ·OH radicals by letting the terephthalic

conventional MIL-53(Fe) but also demonstrate that LMCT mechanism works more effectively, which agrees well with our earlier proposal.

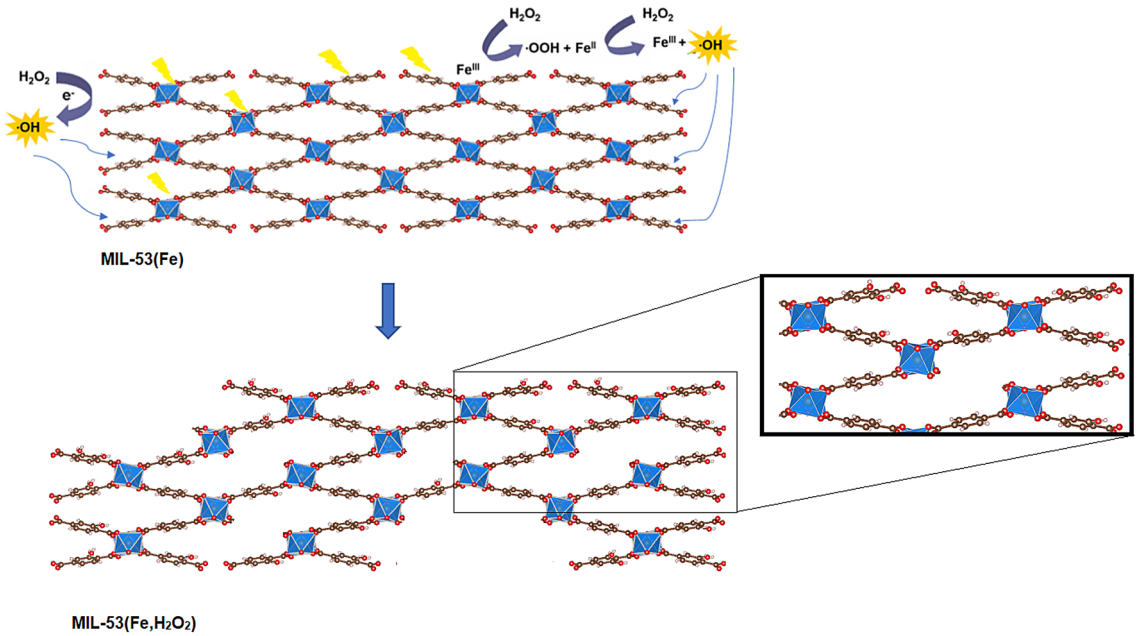

Fig. 6 Proposed mechanism for the modification of MIL-53(Fe) by H_2O_2 under visible light irradiation

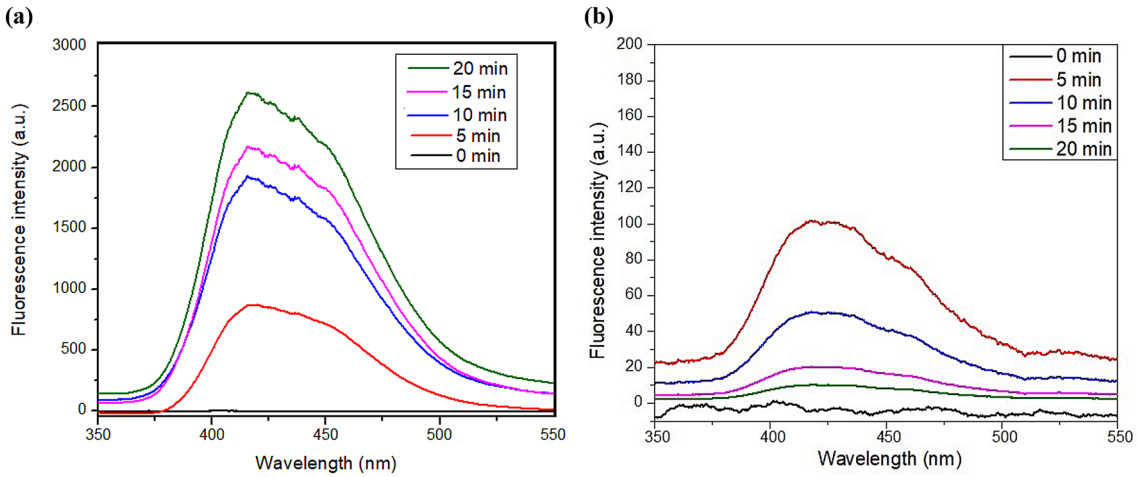

Fig. 7 ·OH-trapping PL spectra of different catalytic systems: **a** MIL-53(Fe, H_2O_2)/vis, **b** MIL-53(Fe)/vis

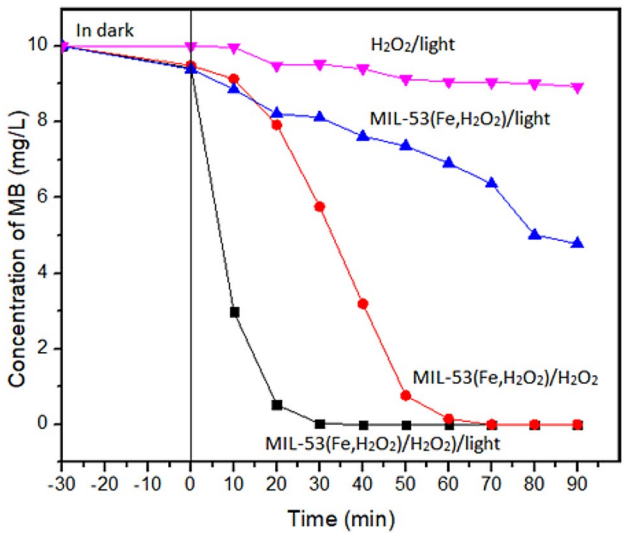

Fig. 8 The degradation of MB in different conditions. (Experimental conditions: MB, 10 mg L^{-1}; H_2O_2, 0.01 mM; and MIL-53(Fe, H_2O_2), 0.2 g L^{-1})

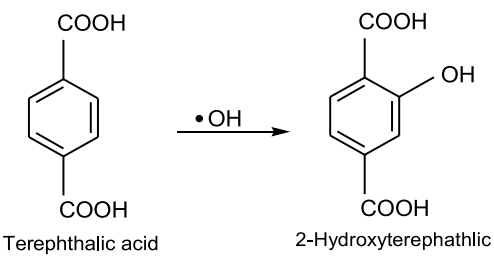

(4)

3.4 Optimization of the experimental Conditions for Photocatalytic Degradation of MB

The degradation of MB was also used to evaluate the catalytic performance of MIL-53(Fe, H_2O_2) in different systems in which pH (*ca.* 7.0) and initial MB concentration of 10 mg L^{-1} was kept constant, the results were illustrated in Fig. 8. After 90 min irradiation, the percentage of MB removal in the presence of MIL-53(Fe, H_2O_2) is 52.2% surpassed the one with H_2O_2 which is 10%. It was mentioned in many previous researches on dye degradation that ·OH radicals created by the H_2O_2 photolysis under visible light ($H_2O_2 + h\nu \rightarrow \cdot OH + OH^-$) caused the reduction of MB concentration. However, it was not effective due to the limited H_2O_2 concentration. In the presence of individual modified MIL-53(Fe), the formation of ·OH was enhanced because of the interaction between MIL-53(Fe, H_2O_2) and H_2O as the solvent based on LMCT mechanism. This interaction increased the degradation efficiency which was discussed in the previous part of this study. Nevertheless, the degradation efficiency of MB in system MIL-53(Fe, H_2O_2)/vis was relatively much lower than that in system MIL-53(Fe, H_2O_2)/H_2O_2/vis. This result proves that the photocatalytic of the modified MIL-53(Fe) still depends on metal–oxo cluster excitation with the external electron receiver H_2O_2. On the other hand, MIL-53(Fe, H_2O_2) is iron-based terephthalate, which suggests that the Fenton-like catalytic process may play the role in the MB decomposition reaction. Therefore, additional experiments in the dark with the presence of H_2O_2 and the modified MIL-53(Fe) was carried out. The required reaction time interval of the experiment in the absence of the visible light was more than twice that of the experiment under visible light, which were within 60 min and 30 min respectively. It indicated that Fenton-liked catalytic processes were not as efficient as photocatalytic processes.

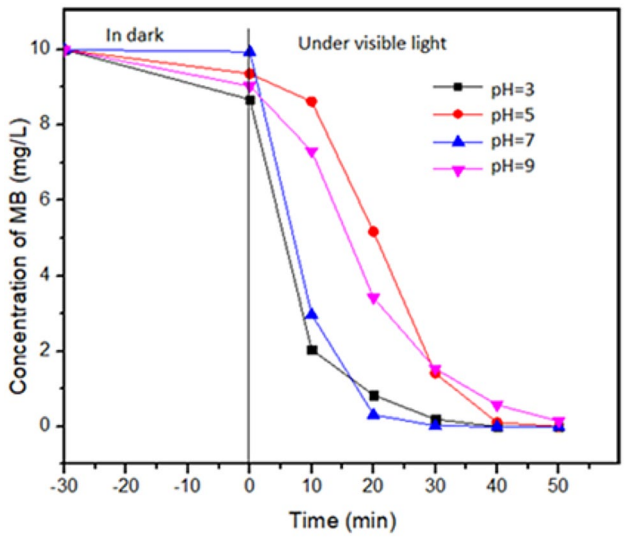

Fig. 9 Effect of initial pH on the degradation of MB. (Experimental conditions: MB, 10 mg L^{-1}; H_2O_2, 0.01 mM; and MIL-53(Fe, H_2O_2), 0.2 g L^{-1})

Furthermore, the effect of pH solution, a crucial parameter that has a great influence on the catalytic reaction, was investigated and the results were shown in Fig. 9. NaOH 1 M solution and 1 M HCl solution were used to adjust pH of the initial MB reaction mixture before adding catalyst. The investigated pH range was from 3.0 to 9.0 for the MIL-53(Fe, H_2O_2)/visible light/H_2O_2 system. The results indicated that the higher was the pH, the lower was the color degradation kinetics. At pH 3, the concentration of MB was significantly reduced to 80% after the first 10 min. This result can be ascribed due to the breakage of MOFs structure inducing free iron ions, which makes the Fenton-like reaction occurs directly without passing electrons through the organic bridging ligands. The kinetics of the reaction at pH 3 was equivalent to that at pH 7. The required reaction time interval at pH 9 was slightly longer, compared to those at other pH values, but almost 100% degradation of MB was attained after 50 min. The reason for this difference might be that H_2O_2 tends to decay to H_2O and oxygen in alkaline solution [26]. The results obtained for activity of the modified MIL-53(Fe) at different pH environments are in good agreement with the previous reports for the original MIL-53(Fe) and Fe-containing MOFs [14, 26, 31, 33].

To examine the effect of H_2O_2 dosage on MB removal over MIL-53(Fe, H_2O_2)/H_2O_2/vis system, experiments with various concentrations of H_2O_2 support were conducted and the results were summarized in Fig. 10a. When H_2O_2 concentration increased from 0.01 to 0.1 mM, the reaction time of the experiments were remained almost unchanged, which was 30 min. This has been explained by Ai et al. that surplus H_2O_2 molecules tap ·OH radicals to produce hydroperoxyl radicals (·OOH) with lower oxidation potential [26, 34]. The required reaction time of the experiment with 0.002 mM H_2O_2 was longer than that with 0.01 mM H_2O_2. However, this process was remarkably enhanced compared to the experiment without H_2O_2 support. These results also demonstrated again that the LCMT mechanism needed supports from metal–oxo cluster excitation and external electron acceptor.

Figure 10b illustrated the effect of as-prepared catalyst concentration over MB degradation experiments. The concentration of MB was adjusted in the range of 0.1–0.4 g L^{-1}, and the amount of solid powder was set from 5 to 20 mg. When catalyst concentration increased from 0.2 to 0.4 g L^{-1}, the degradation efficiency was slightly changed but the degradation time remained almost constant, suggesting that the

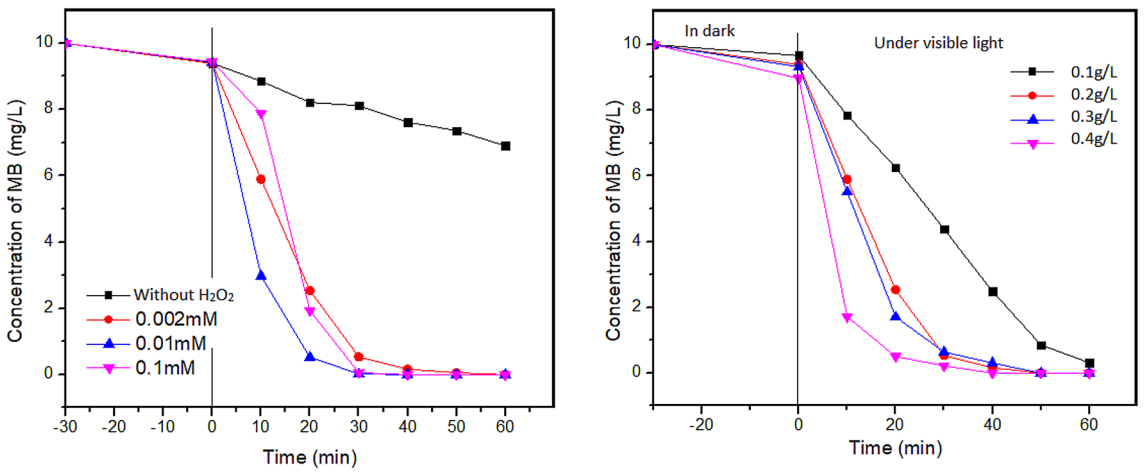

Fig. 10 **a** Effect of H_2O_2 concentration and **b** catalyst concentration on the degradation of MB over MIL-53(Fe, H_2O_2)/visible light/H_2O_2 system. Experimental conditions: MB, 10 mg L^{-1}; MIL-53(Fe, H_2O_2), 0.2 g L^{-1}; and initial pH 7

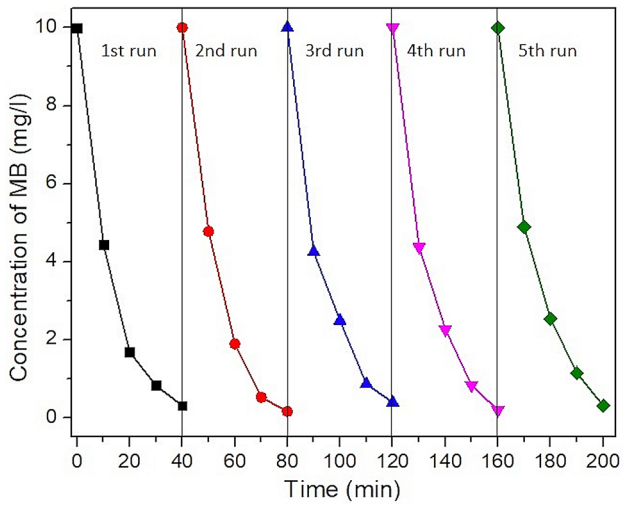

Fig. 11 Recycling and reuse of MIL-53(Fe, H_2O_2) photocatalyst for the removal of methylene blue. (Experimental conditions: MB, 10 mg L^{-1}; H_2O_2, 0.01 mM; and MIL-53(Fe, H_2O_2), 0.2 g L^{-1})

·OH was insignificantly improved. Meanwhile, the degradation efficiency was reduced if the catalyst concentration was decreased to 0.1 g L^{-1}, and MB was completely decomposed within 60 min. In general, with the initial MB concentration of 10 mg L^{-1}, the appropriate amount of catalyst was 0.2 g L^{-1} or 10 mg of modified MIL-53(Fe) solid powder.

3.5 Recycling and Reuse of Modified MIL-53(Fe) Photocatalyst for the Removal of Methylene Blue

To determine the stability of MIL-53(Fe, H_2O_2), the material was recovered from the resulting MB aqueous by centrifugation and reused for subsequent reactions. The result of reusing of modified MIL-53(Fe) photocatalyst for the removal of methylene blue is shown in Fig. 11. It is noticeable that modified MIL-53(Fe) photocatalyst had photocatalytic stability for the removal of methylene blue for five times at least.

Table 3 Physical properties and photocatalytic performance of some modified MOFs

Photocatalyst (mg)	Modification method	Bandgap (eV)	S_{BET} (m^2 g^{-1})	Photodegradation experiments					
				Light source (W)	Pollutant (mg L^{-1})	H_2O_2 concentration (mM)	Degradation rate (time min)	Cycles	References
MIL-53(Fe) (10)	None	2.88	19.1	Halogen tungsten lamp (500)	RhB (10)	20	100% (50 min)	3	[26]
MIL-53(Fe)	Microwave-assistance	2.8	–	Xenon lamp (300)	MB (15)	Use H_2O_2 No use H_2O_2	100% (90 min) 50% (90 min)	–	[17]
MIL-53(Fe, H_2O_2) (10)	Modified linkers	2.25	8.93	Halogen tungsten lamp (500)	MB (10)	0.01	100% (40 min)	5	This study
NH_2-MIL-53(Fe)	Modified linkers	2.59	–	–	–	–	–	–	[40]
NH_2-MIL-88B(Fe) (50)	Modified linkers	1.14	–	Xenon lamp (500)	MB (30)	100 µL H_2O_2 30%	57% (120 min)	–	[41]
g-C_3N_4/NH_2-MIL-88B(Fe) (50)	Modified likers & nanocomposite	–	–	Xenon lamp (500)	MB (30)	100 µL H_2O_2 30%	100% (120 min)	4	[41]
Fe_3O_4/MIL-53(Fe)	Nanocomposite	–	–	Halogen tungsten lamp (500)	RhB (10)	20	100% (70 min)	3	[20]
g-C_3N_4/MIL-53(Fe)	Nanocomposite	2.51	18.5	Xenon lamp (500)	Cr^{VI} (10 ppm)	No use H_2O_2	100% (180 min)	4	[22]
$NiFe_2O_4$/MIL-53(Fe) (20)	Nanocomposite	–	43.49	Compact fluoresence lamp (40)	RhB (3.10^{-5} M)	0.01	95% (180 min)	-	[42]
CdS/MIL-53(Fe) (75)	Nanocomposite	2.27	20.879	Oreva CFL bulb (85)	KTC (10)	No use H_2O_2	80% (330 min)	3	[39]

As a comparison, the modified MIL-53(Fe) showed the exhibiting the highest photocatalytic activity for methylene blue degradation under visible-light irradiation (Table 3).

4 Conclusion

This study provides a facile way to modify MIL-53(Fe) catalyst and its photochemical insights. The degradation experiments along with FL spectroscopic studies have confirmed the catalytic activity enhancement resulted from the proposed modification step. The XRD results showed that the material structure changed to amorphous phases and the photocatalytic efficiency was improved after modified by H_2O_2. The MIL-53(Fe, H_2O_2) nanoparticles about 100–300 nm in size was successfully prepared and confirmed by SEM images. In term of UV–Vis DRS results, the absorption spectrum of modified MIL-53(Fe) shifted to higher wavelength and the calculated band gap of the modified MIL-53(Fe) is 2.2 eV, which is lower than the value of the conventional one. More efforts are being made to improve the stability of the final product and put a stop to the dependence on external H_2O_2 support. MIL-53(Fe, H_2O_2) is a promising catalyst which can be used for other oxidation reactions based on the formation of ·OH agents.

Acknowledgements This research was funded by the Vietnam National Foundation for Science and Technology Development (NAFOSTED) under Grant Number 104.01-2014.47.

Compliance with Ethical Standards

Conflict of interest The authors declare that they have no conflict of interest.

References

1. Yılmaz E, Sert E, Atalay FS (2016) Synthesis, characterization of a metal organic framework: MIL-53 (Fe) and adsorption mechanisms of methyl red onto MIL-53 (Fe). J Taiwan Inst Chem Eng 65:323–330
2. Robinson T, Chandran B, Nigam P (2002) Removal of dyes from a synthetic textile dye effluent by biosorption on apple pomace and wheat straw. Water Res 36:2824–2830
3. Bennett TD, Cheetham AK (2014) Amorphous metal–organic frameworks. Acc Chem Res 47:1555–1562
4. Bennett TD, Horike S (2018) Liquid, glass and amorphous solid states of coordination polymers and metal–organic frameworks. Nat Rev Mater 3:431–440
5. Bennett TD, Keen DA, Tan J-C, Barney ER, Goodwin AL, Cheetham AK (2011) Thermal amorphization of zeolitic imidazolate frameworks. Angew Chem Int Ed 50:3067–3071
6. Guillerm V, Ragon F, Dan-Hardi M, Devic T, Vishnuvarthan M, Campo B et al (2012) A series of isoreticular, highly stable, porous zirconium oxide based metal–organic frameworks. Angew Chem Int Ed Engl 51:9267–9271
7. Chapman KW, Sava DF, Halder GJ, Chupas PJ, Nenoff TM (2011) Trapping guests within a nanoporous metal–organic framework through pressure-induced amorphization. J Am Chem Soc 133:18583–18585
8. Conrad S, Kumar P, Xue F, Ren L, Henning S, Xiao C et al (2018) Controlling dissolution and transformation of zeolitic imidazolate frameworks by using electron-beam-induced amorphization. Angew Chem Int Ed 57:13592–13597
9. Jiang D, Xu P, Wang H, Zeng G, Huang D, Chen M et al (2018) Strategies to improve metal organic frameworks photocatalyst's performance for degradation of organic pollutants. Coord Chem Rev 376:449–466
10. Araya T, Jia M, Yang J, Zhao P, Cai K, Ma W et al (2017) Resin modified MIL-53(Fe) MOF for improvement of photocatalytic performance. Appl Catal B 203:768–777
11. Llewellyn PL, Horcajada P, Maurin G, Devic T, Rosenbach N, Bourrelly S et al (2009) Complex adsorption of short linear alkanes in the flexible metal–organic-framework MIL-53(Fe). J Am Chem Soc 131:13002–13008
12. El Osta R, Carlin-Sinclair A, Guillou N, Walton RI, Vermoortele F, Maes M et al (2012) Liquid-phase adsorption and separation of xylene isomers by the flexible porous metal–organic framework MIL-53(Fe). Chem Mater 24:2781–2791
13. Jia J, Xu F, Long Z, Hou X, Sepaniak MJ (2013) Metal-organic framework MIL-53(Fe) for highly selective and ultrasensitive direct sensing of MeHg(+). Chem Commun 49:15
14. Du JJ, Yuan YP, Sun JX, Peng FM, Jiang X, Qiu LG et al (2011) New photocatalysts based on MIL-53 metal–organic frameworks for the decolorization of methylene blue dye. J Hazard Mater 190:945–951
15. Hu C, Huang Y-C, Chang A-L, Nomura M (2019) Amine functionalized ZIF-8 as a visible-light-driven photocatalyst for Cr(VI) reduction. J Colloid Interface Sci 553:372–381
16. Nikseresht A, Daniyali A, Ali-Mohammadi M, Afzalinia A, Mirzaie A (2017) Ultrasound-assisted biodiesel production by a novel composite of Fe(III)-based MOF and phosphotangestic acid as efficient and reusable catalyst. Ultrasonics Sonochem 37:203–207
17. Trinh ND, Hong SS (2015) Photocatalytic decomposition of methylene blue over MIL-53(Fe) prepared using microwave-assisted process under visible light irradiation. J Nanosci Nanotechnol 15:5450–5454
18. Dao X-Y, Xie X-F, Guo J-H, Zhang X-Y, Kang Y-S, Sun W-Y (2020) Boosting photocatalytic CO_2 reduction efficiency by heterostructures of NH2-MIL-101(Fe)/g-C3N4. ACS Appl Energy Mater 3:3946–3954
19. Lin R, Li S, Wang J, Xu J, Xu C, Wang J et al (2018) Facile generation of carbon quantum dots in MIL-53(Fe) particles as localized electron acceptors for enhancing their photocatalytic Cr(VI) reduction. Inorg Chem Front 5:3170–3177
20. Zhang C, Ai L, Jiang J (2015) Solvothermal synthesis of MIL–53(Fe) hybrid magnetic composites for photoelectrochemical water oxidation and organic pollutant photodegradation under visible light. J Mater Chem A 3:3074–3081
21. Liang R, Shen L, Jing F, Qin N, Wu L (2015) Preparation of MIL-53(Fe)-reduced graphene oxide nanocomposites by a simple self-assembly strategy for increasing interfacial contact: efficient visible-light photocatalysts. ACS Appl Mater Interfaces 7:9507–9515
22. Huang W, Liu N, Zhang X, Wu M, Tang L (2017) Metal organic framework g-C3N4/MIL-53(Fe) heterojunctions with enhanced photocatalytic activity for Cr(VI) reduction under visible light. Appl Surf Sci 425:107–116
23. Xiang W, Zhang Y, Lin H, Liu CJ (2017) Nanoparticle/metal–organic framework composites for catalytic applications: current status and perspective. Molecules 22:30

24. Cai X, Xie Z, Li D, Kassymova M, Zang S-Q, Jiang H-L (2020) Nano-sized metal–organic frameworks: synthesis and applications. Coord Chem Rev 417:213366
25. Nguyen M-TH, Nguyen Q-T (2014) Efficient refinement of a metal–organic framework MIL-53(Fe) by UV–Vis irradiation in aqueous hydrogen peroxide solution. J Photochem Photobiol, A 288:55–59
26. Ai L, Zhang C, Li L, Jiang J (2014) Iron terephthalate metal–organic framework: revealing the effective activation of hydrogen peroxide for the degradation of organic dye under visible light irradiation. Appl Catal B 148–149:191–200
27. He J, Zhang Y, Zhang X, Huang Y (2018) Highly efficient Fenton and enzyme-mimetic activities of NH2-MIL-88B(Fe) metal organic framework for methylene blue degradation. Sci Rep 8:5159
28. Qu X, Kirschenbaum LJ, Borish ET (2000) Hydroxyterephthalate as a fluorescent probe for hydroxyl radicals: application to hair melanin. Photochem Photobiol 71:307–313
29. Vu TA, Le GH, Dao CD, Dang LQ, Nguyen KT, Nguyen QK et al (2015) Arsenic removal from aqueous solutions by adsorption using novel MIL-53(Fe) as a highly efficient adsorbent. RSC Adv 5:5261–5268
30. Liang R, Jing F, Shen L, Qin N, Wu L (2015) MIL-53(Fe) as a highly efficient bifunctional photocatalyst for the simultaneous reduction of Cr(VI) and oxidation of dyes. J Hazard Mater 287:364–372
31. Alvaro M, Carbonell E, Ferrer B, Llabres i Xamena FX, Garcia H (2007) Semiconductor behavior of a metal–organic framework (MOF). Chemistry 13:5106–5112
32. De Vos A, Hendrickx K, Van Der Voort P, Van Speybroeck V, Lejaeghere K (2017) Missing linkers: an alternative pathway to UiO-66 electronic structure engineering. Chem Mater 29:3006–3019
33. Wang D, Huang R, Liu W, Sun D, Li Z (2014) Fe-based MOFs for photocatalytic CO_2 reduction: role of coordination unsaturated sites and dual excitation pathways. ACS Catal 4:4254–4260
34. Chen Q, Wu P, Li Y, Zhu N, Dang Z (2009) Heterogeneous photo-Fenton photodegradation of reactive brilliant orange X-GN over iron-pillared montmorillonite under visible irradiation. J Hazard Mater 168:901–908
35. Pu M, Guan Z, Ma Y, Wan J, Wang Y, Brusseau ML et al (2018) Synthesis of iron-based metal-organic framework MIL-53 as an efficient catalyst to activate persulfate for the degradation of Orange G in aqueous solution. Appl Catal A 549:82–92
36. Li X, Guo W, Liu Z, Wang R, Liu H (2016) Fe-based MOFs for efficient adsorption and degradation of acid orange 7 in aqueous solution via persulfate activation. Appl Surf Sci 369:130–136
37. Panda R, Rahut S, Basu JK (2016) Preparation of a Fe2O3/MIL-53(Fe) composite by partial thermal decomposition of MIL-53(Fe) nanorods and their photocatalytic activity. RSC Adv 6:80981–80985
38. Nguyen V, Nguyen T, Bach L, Hoang T, Bui Q, Tran L et al (2018) Effective photocatalytic activity of mixed Ni/Fe-base metal–organic framework under a compact fluorescent daylight lamp. Catalysts 8:487
39. Chaturvedi G, Kaur A, Kansal SK (2019) CdS-decorated MIL-53(Fe) microrods with enhanced visible light photocatalytic performance for the degradation of ketorolac tromethamine and mechanism insight. J Phys Chem C 123:16857–16867
40. Xu X, Li J, Li Y, Ni B, Liu X, Pan L (2018) Chapter 4: selection of carbon electrode materials. In: Ahualli S, Delgado ÁV (eds) Interface Science and Technology. Elsevier, Amsterdam, pp 65–83
41. Li X, Pi Y, Wu L, Xia Q, Wu J, Li Z et al (2017) Facilitation of the visible light-induced Fenton-like excitation of H2O2 via heterojunction of g-C_3N_4/NH_2-iron terephthalate metal-organic framework for MB degradation. Appl Catal B 202:653–663
42. Nguyen VH, Bach LG, Bui QTP, Nguyen TD, Vo D-VN, Vu HT et al (2018) Composite photocatalysts containing MIL-53(Fe) as a heterogeneous photo-Fenton catalyst for the decolorization of rhodamine B under visible light irradiation. J Environ Chem Eng 6:7434–7441

Publisher's Note Springer Nature remains neutral with regard to jurisdictional claims in published maps and institutional affiliations.